Physica **44** (1969) 273–290

THE SLIP SYSTEMS IN KCl : Pb

A PIEZOSPECTROSCOPIC INVESTIGATION OF THE Pb^{++} CENTRE

P. KOEZE* and J. VOLGER

Fysisch Laboratorium der Rijksuniversiteit, Utrecht, Nederland

Received 13 January 1969

Synopsis

The stress-induced polarization of the luminescence of KCl:Pb is determined. It reveals the many possible slip systems in KCl. If the uniaxial stress is applied along ⟨100⟩ the frequently observed $\{1\bar{1}0\}\langle 110\rangle$ systems are stressed. In general, at low stresses one or two of the four stressed systems are active (orthogonal slip), at high stresses all four stressed systems are active (oblique slip). If the uniaxial stress is applied along ⟨111⟩ it is highly probable that one of the three stressed {001}⟨110⟩ systems is active. A uniaxial stress along ⟨110⟩ can produce slip in many different ways. If the sample has a nearly quadratic cross section two or four $\{1\bar{1}0\}\langle 110\rangle$ systems are active, if the sample is uncommonly shaped it is possible to force slip on one, two, three, or even four {001}⟨110⟩ systems.

1. *Introduction.* In an earlier paper[1]) we determined the Pb^{++} centre in KCl to consist of a substitutional Pb^{++} ion and a K^+ vacancy at a next-nearest neighbour site, the whole centre having the symmetry 4mm. The first excited level of the Pb^{++} ion $^3P_1$ has split into two sublevels, a lower doublet with E symmetry, and a higher singlet with A_2 symmetry. Absorption occurs between the ground level $^1S_0$ and the two excited sublevels, emission occurs only from the lowest E level. The double degeneracy of the E level may be removed by mechanical deformation of the KCl lattice, a procedure generally known as piezospectroscopy[2,3]). If the bands would be sharp enough the splitting could be seen with a spectrograph with a great dispersion. This has been done for zero-phonon lines in a great number of colour centre spectra. But as the emission band is wide, the very small splitting cannot be observed in the emission spectrum. The polarization degree of the emitted radiation, however, is a function of the applied compressive uniaxial stress and, in fact, can be measured. As will be shown, the stress-induced polarization reveals the many possible slip systems in KCl.

* Now at the Bataafse Internationale Petroleum Maatschappij N.V., 's-Gravenhage, Nederland.

2. *Experimental.* Single crystals of lead-doped KCl were obtained from Dr. K. Korth, Kiel, West-Germany. The Pb^{++} concentration was according to the manufacturer 10^{-3} molar fraction. We measured the absorption coefficient at 272 nm and room temperature, and found it to be 8.7×10^3 m^{-1}. According to Sibley *et al.*[4]) this corresponds to a Pb^{++} concentration of 5×10^{-5} molar fraction. No precipitation was observed with the optical microscope. The dimensions of the samples were about $3 \times 6 \times 8$ mm^3. Samples with {100} faces were cleft, samples with {110}, {111}, and {112} faces were polished on wet silk tightened on a glass plate, a method already described by Grailich in 1858[5]).

After the preparation and before each measurement the samples were annealed at 630°C for 20 min and then slowly colled down to room temperature at a rate of about 1°C min^{-1}. We used as controller a Leeds and Northrup Speedomax H recorder with 2-action D.A.T. control unit for cam type programme control, and as furnace a 400 W Heraeus furnace. All stresses induced during cleaving and polishing, and by pressing had vanished after annealing. As the faces of KCl : Pb crystals are thermally etched at temperatures above 600°C[6]), special precautions had to be taken to avoid the damage of the optical surfaces. We therefore placed the samples with the faces on flat, polished fused silica plates.

For measuring the small changes in the polarization degree with a high accuracy we used a sensitive differential polarimeter. An extensive description is given in ref. 6. The sensitivity in these experiments is about 10^{-4}.

The piezospectroscopic studies were made with the arrangement given in fig. 1. The ultraviolet radiation from a deuterium lamp is focused on a sample through a $NiSO_4$-filter ($NiSO_4.6H_2O$, 500 kg m^{-3}, 10 mm). The sample is placed in a hydraulic crystal press, the force being applied in the vertical

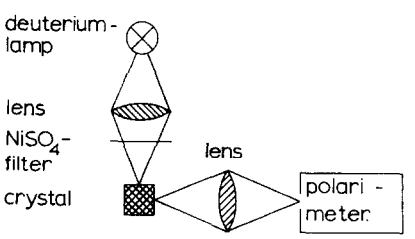

Fig. 1. Optical arrangement for measuring the piezospectroscopic effect.

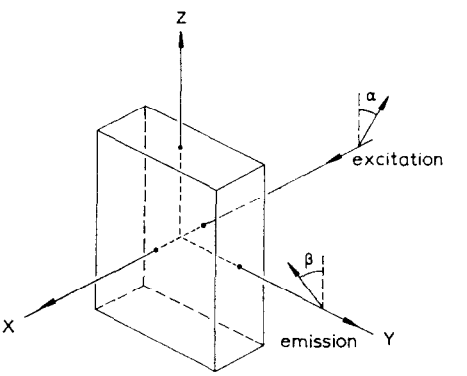

Fig. 2. The directions of the exciting and the emitted radiation with respect to the sample orientation. The uniaxial stress is applied along the z axis.

direction perpendicular to the plane of the figure. The emitted radiation is focussed onto the slit of the polarimeter. The samples are mounted in the press with thin rubber sheets between the crystal surfaces and the stamps of the press. To avoid friction the rubber sheets are powdered with talcum powder. We calibrated the press with the stress birefringence induced in dummy crystals (CIBA Araldite B(CT200), hardener HT901). The reproducibility of the exerted force is 3×10^{-2} at high forces. Föppl and Mönch [7]) give a detailed description of the method. The stress is distributed uniformly on the crystal surfaces as could be ascertained with the dummy crystals. The valves of the hydraulic press were opened always very carefully to prevent overloading of the crystals. We used an optical filter (Jena UG 12, 4 mm thick) in the polarimeter to eliminate possible stray light.

The sample orientation is illustrated in fig. 2. The crystal was excited by radiation incident along the x axis, the detection apparatus was placed along the y axis, the compressive uniaxial stress was applied along the z axis. We define the polarization degree P of the detected radiation as:

$$P = \frac{I_Z - I_X}{I_Z + I_X}, \tag{1}$$

where I_Z is the intensity of the radiation with the electric vector along the z axis and I_X is the intensity with the electric vector along the x axis. The longest dimension of the rectangular sample was always directed along the z axis, the shortest dimension always along the x axis.

3. *Results and evaluation.* In figs. 3 and 4 the piezospectroscopic effect of KCl : Pb, *i.e.* the difference in the polarization degree of the emitted radiation when the crystal is loaded and unloaded, is given. Generally, there is a linear relationship between the polarization degree and the stress, the flow stress is marked by a discontinuity. The uniaxial stress splitting of doubly degenerated E states of the tetragonal centres in cubic crystals has been investigated by Hughes and Runciman [3]). In the following we have drawn heavily on their results.

A simple calculation shows that unpolarized rediation excites the E level of the three different oriented tetragonal centres equally well. In fig. 5 the level scheme is drawn according to which the E level is split under a uniaxial stress σ in the elastic region. A_1, A_2, B, and C are the piezospectroscopic constants as defined by Hughes and Runciman; A_1 and A_2 describe the splitting of the orientationally degenerated levels, while B and C characterize the splitting of the electronically degenerated levels. As far as the splitting of the excited states originates from an electronic degeneracy there is a Boltzmann distribution over the levels, but as far as the splitting originates from an ionic degeneracy the states are equally populated, as the frequency

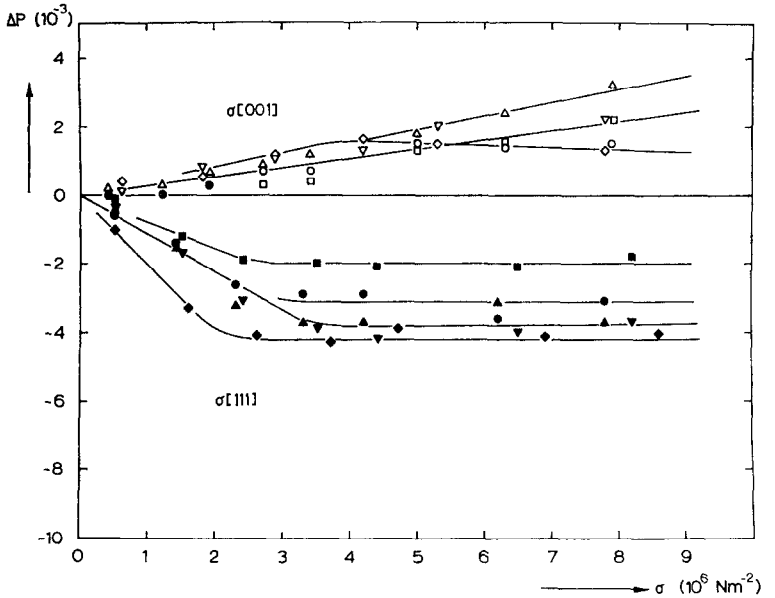

Fig. 3. The piezospectroscopic effect with the stress σ applied along [001] and along [111]. The [111] effect is independent of the observation axis chosen, *viz.* [1$\bar{1}$0] and[11$\bar{2}$].

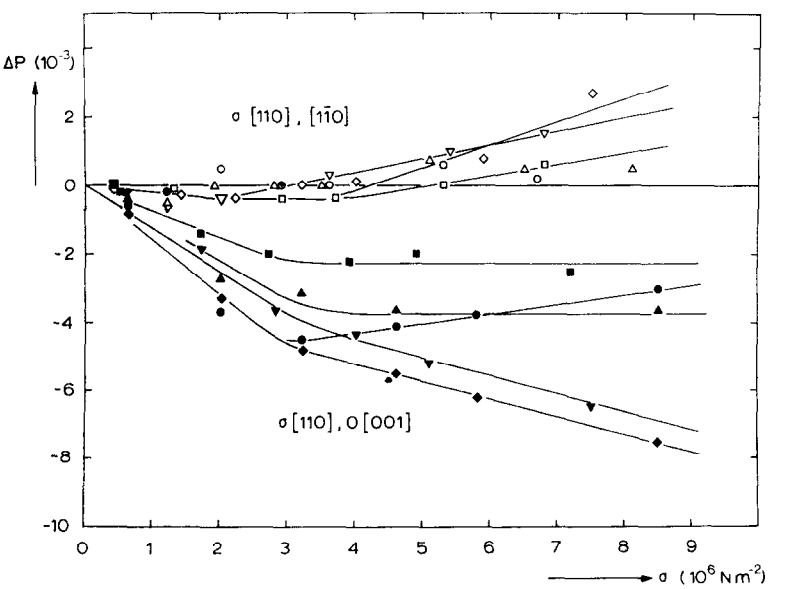

Fig. 4. The piezospectroscopic effect with the stress σ applied along [110]. The luminescence is observed along [1$\bar{1}$0] and [001].

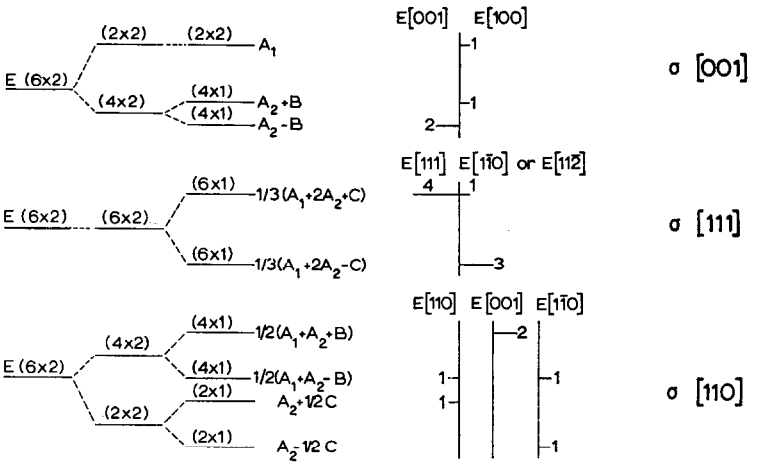

Fig. 5. The stress splitting of an E level. The numbers between parentheses denote the product of the orientational and electronic degeneracy of each level, the energy shifts are given beside the levels.
At the right hand of the figure the polarization of the emitted radiation along the axis of observation, the electric vector being perpendicular and parallel to the applied stress.

for reorientation of the centres is very low at room temperature[9,10]). Thus, only B and C will appear in the stress-dependent polarization degree P.

$$\sigma[001], \qquad P = \frac{2\exp(B\sigma/k\theta) - \exp(-B\sigma/k\theta) - 1}{4}. \tag{2}$$

$$\text{If} \quad P = a\sigma, \qquad \text{then} \qquad B = \tfrac{4}{3}ak\theta. \tag{3}$$

$$\sigma[111] \qquad P = \frac{3\exp(-C\sigma/3k\theta) - 3\exp(C\sigma/3k\theta)}{8}. \tag{4}$$

$$\text{If} \quad P = b\sigma, \qquad \text{then} \qquad C = -4bk\theta. \tag{5}$$

$$\sigma[110], 0[1\bar{1}0] \quad P = \frac{\exp(B\sigma/2k\theta) - 2\exp(-B\sigma/2k\theta) + \exp(-C\sigma/2k\theta)}{4}. \tag{6}$$

$$\text{If} \quad P = c\sigma, \qquad \text{then} \qquad 3B - C = 8ck\theta. \tag{7}$$

$$\sigma[110], 0[001] \quad P = \frac{\exp(-C\sigma/2k\theta) - \exp(C\sigma/2k\theta)}{4}. \tag{8}$$

$$\text{If} \quad P = d\sigma, \qquad \text{then} \qquad C = -4dk\sigma. \tag{9}$$

Here k is the Boltzmann constant, θ is the absolute temperature, a, b, c and d are experimental constants. The constants a, b, c and d are found according to figs. 3 and 4, within the following intervals:

$$\begin{aligned} a&: \quad (+\ 1.5 - +4.5\ ) \times 10^{-10}\ \mathrm{m^2\ N^{-1}},\\ b&: \quad (-20 \quad - -8\ \ ) \times 10^{-10}\ \mathrm{m^2\ N^{-1}},\\ c&: \quad (-\ 4 \quad -\ \ 0\ \ ) \times 10^{-10}\ \mathrm{m^2\ N^{-1}},\\ d&: \quad (-17 \quad - -7\ \ ) \times 10^{-10}\ \mathrm{m^2\ N^{-1}}. \end{aligned} \tag{10}$$

Theoretically, the stress splitting is given by the two constants B and C. Experimentally, however, we determined four constants: a, b, c and d. Thus, there must be two conditions which interrelate the four experimental constants. From eqs. (5) and (9) it follows that

$$b = d \tag{11}$$

and from eqs. (3), (5) and (7) that

$$a + b = 2c. \tag{12}$$

If conditions (11) and (12) are to be fulfilled we must take:

$$\begin{aligned} a &= +(3.0 \pm 1.5) \times 10^{-10}\ \mathrm{m^2\ N^{-1}},\\ b &= -(9.5 \pm 1.5) \times 10^{-10}\ \mathrm{m^2\ N^{-1}},\\ c &= -(3.3 \pm 0.8) \times 10^{-10}\ \mathrm{m^2\ N^{-1}},\\ d &= -(9.5 \pm 1.5) \times 10^{-10}\ \mathrm{m^2\ N^{-1}}. \end{aligned} \tag{13}$$

With eqs. (3) and (5) we obtain, if $k\theta = 0.025$ eV,

$$\begin{aligned} B &= +(1.0 \pm 0.5) \times 10^{-11}\ \mathrm{eV\ m^2\ N^{-1}},\\ C &= +(9.5 \pm 1.5) \times 10^{-11}\ \mathrm{eV\ m^2\ N^{-1}}. \end{aligned} \tag{14}$$

At stresses exceeding the flow stress σ_f the samples are plastically deformed and internal stresses are left behind in the crystal after the load is taken away. These internal stresses cause a piezospectroscopic effect even if $\sigma = 0$. As it is impossible to measure the absolute value of the polarization degree with the polarimeter, we recorded the difference in the polarization degree of the loaded crystal P_σ and of the unloaded crystal P_0. In the loaded crystal the stress is uniformly distributed over the whole volume and Hooke's law is valid up to high stresses. So, P_σ is known by extrapolation of the measurements in the elastic region. On the other hand, the polarization degree of the emitted radiation for an unloaded crystal P_0 might be calculated if the magnitude of the residual shear stresses and the activated slip systems were known. Making a sensible assumption on the magnitude, we can compute P_0 for any possible set of slip systems. The results of these computations for all relevant cases are given in the tables I up to XV. The first column gives the direction along which the stress σ is applied. Column 2 gives the possible

TABLE I

axis of compression	slip system	shear stress τ	tensor elements σ_{ij}	energy shifts Δ	state of polarization E[001]	state of polarization E[100]	zero-load polarization P_0
					E[001]	E[100]	
	$(\bar{1}01)$ $[101]$		$\sigma_x = -\tau_r$	$A_1 - A_2 + B$	0	0	
			$\sigma_y = 0$	$A_1 - A_2 - B$	0	2	
[001]	or	$\frac{1}{2}\sigma$[001]	$\sigma_z = +\tau_r$	$+ 2B$	1	1	0
			$\tau_{xy} = \tau_{xz} = \tau_{yz} = 0$	$- 2B$	1	1	
	(101) $[\bar{1}01]$			$-A_1 + A_2 + B$	0	0	
				$-A_1 + A_2 - B$	2	0	

TABLE II

					E[001]	E[100]	
			$\sigma_x = -2\tau_r$				
	$(\bar{1}01)$ $[101]$		$\sigma_y = -2\tau_r$	$4A_1 - 4A_2$	0	1	$\frac{9B\tau_r}{2k\Theta}$
[001]	(101) $[\bar{1}01]$	$\frac{1}{2}\sigma$[001]	$\sigma_z = +4\tau_r$	$-2A_1 + 2A_2 + 6B$	0	1	
	$(0\bar{1}1)$ $[011]$		$\tau_{xy} = \tau_{xz} = \tau_{yz} = 0$	$-2A_1 + 2A_2 - 6B$	2	0	
	(011) $[0\bar{1}1]$						

TABLE III

					E[111]	E[1$\bar{1}$0]	E[11$\bar{2}$]	
	$(1\bar{1}1)$ $[110]$		$\sigma_x = \sigma_y = \sigma_z = 0$					
	$(\bar{1}11)$ $[101]$		$\tau_{xy} = \frac{1}{3}\sqrt{6}\,\tau_r$	$+\frac{1}{3}\sqrt{6}\,C$	4	1	1	
[111]	$(11\bar{1})$ $[001]$	$\frac{1}{9}\sqrt{6}\,\sigma$[111]	$\tau_{xz} = \frac{1}{3}\sqrt{6}\,\tau_r$					$\frac{-\sqrt{6}\,C\tau_r}{4k\Theta}$
	or		$\tau_{yz} = \frac{1}{3}\sqrt{6}\,\tau_r$	$-\frac{1}{3}\sqrt{6}\,C$	0	3	3	
	$(\bar{1}11)$ $[110]$							
	$(11\bar{1})$ $[101]$							
	$(1\bar{1}1)$ $[011]$							

TABLE IV

axis of compression	slip system	shear stress τ	tensor elements σ_{ij}	energy shifts Δ	state of polarization E[111]	E[1$\bar{1}$0]	E[11$\bar{2}$]	zero-load polarization P_0
			$\sigma_x = \sigma_y = \sigma_z = 0$					
	(001) [110]		$\tau_{xy} = \sqrt{2}\,\tau_r$	$+\sqrt{2}\,C$	4	1	1	$-\frac{3\sqrt{2}\,C\tau_r}{4k\Theta}$
[111]	(010) [101]	$\frac{1}{3}\sqrt{2}\,\sigma$[111]	$\tau_{xz} = \sqrt{2}\,\tau_r$	$-\sqrt{2}\,C$	0	3	3	
	(100) [011]		$\tau_{yz} = \sqrt{2}\,\tau_r$					

TABLE V

axis of compression	slip system	shear stress τ	tensor elements σ_{ij}	energy shifts Δ	state of polarization E[111]	E[1$\bar{1}$0]	E[11$\bar{2}$]	zero-load polarization P_0
			$\sigma_x = \sigma_y = \sigma_z = 0$					0[1$\bar{1}$0]:
				$-\frac{1}{2}\sqrt{2}\,C$	16	6	2	$-\frac{\sqrt{2}\,C\tau_r}{3k\Theta}$
[111]	(001) [110]	$\frac{1}{3}\sqrt{2}\,\sigma$[111]	$\tau_{xy} = 0$	0	8	12	4	
			$\tau_{xz} = \frac{1}{2}\sqrt{2}\,\tau_r$	$-\frac{1}{2}\sqrt{2}\,C$	0	6	18	0[11$\bar{2}$]:
			$\tau_{yz} = \frac{1}{2}\sqrt{2}\,\tau_r$					$-\frac{\sqrt{2}\,C\tau_r}{6k\Theta}$

TABLE VI

axis of compression	slip system	shear stress τ	tensor elements σ_{ij}	energy shifts Δ	state of polarization E[111]	E[1$\bar{1}$0]	E[11$\bar{2}$]	zero-load polarization P_0
	(010) [101]		$\sigma_x = \sigma_y = \sigma_z = 0$					0[1$\bar{1}$0]:
			$\tau_{xy} = \frac{1}{2}\sqrt{2}\,\tau_r$	$+\frac{1}{2}\sqrt{2}\,C$	16	3	5	$-\frac{5\sqrt{2}\,C\tau_r}{24k\Theta}$
[111]	or	$\frac{1}{3}\sqrt{2}\sigma$[111]		0	8	6	10	
			$\tau_{xz} = 0$ or $\frac{1}{2}\sqrt{2}\tau_1$	$-\frac{1}{2}\sqrt{2}\,C$	0	15	9	
	(100) [011]		$\tau_{yz} = \frac{1}{2}\sqrt{2}\,\tau_r$ or 0					0[11$\bar{2}$]:
								$-\frac{7\sqrt{2}\,C\tau_r}{24k\Theta}$

TABLE VII

axis of compression	slip system	shear stress τ	tensor elements σ_{ij}	energy shifts Δ	state of polarization E[111]	E[1$\bar{1}$0]	E[11$\bar{2}$]	zero-load polarization P_0
			$\sigma_x = \sigma_y = \sigma_z = 0$					0[1$\bar{1}$0]:
	(100) [011]		$\tau_{xy} = \sqrt{2}\,\tau_r$	$+\sqrt{2}\,C$	8	0	4	$-\frac{5\sqrt{2}\,C\tau_r}{12k\Theta}$
[111]	(010) [101]	$\frac{1}{3}\sqrt{2}\,\sigma$[111]	$\tau_{xz} = \frac{1}{2}\sqrt{2}\,\tau_r$	$+\frac{1}{2}\sqrt{2}\,C$	16	6	2	
				$-\frac{1}{2}\sqrt{2}\,C$	0	6	18	
			$\tau_{yz} = \frac{1}{2}\sqrt{2}\,\tau_r$	$-\sqrt{2}\,C$	0	12	0	0[11$\bar{2}$]: $-\frac{7\sqrt{2}\,C\tau_r}{12k\Theta}$

TABLE VIII

					E[111]	E[1$\bar{1}$0]	E[11$\bar{2}$]	
	(100) [011]		$\sigma_x = \sigma_y = \sigma_z = 0$					0[1$\bar{1}$0]:
	(001) [110]			$+\sqrt{2}\,C$	8	3	1	$-\frac{13\sqrt{2}\,C\tau_r}{24k\Theta}$
[111]	or	$\frac{1}{3}\sqrt{2}\,\sigma$[111]	$\tau_{xy} = \frac{1}{2}\sqrt{2}\,\tau_r$	$+\frac{1}{2}\sqrt{2}\,C$	16	3	5	
	(010) [101]		$\tau_{xz} = \sqrt{2}\,\tau_r$ or $\frac{1}{2}\sqrt{2}\,\tau_r$	$-\frac{1}{2}\sqrt{2}\,C$	0	15	9	0[11$\bar{2}$]:
	(001) [110]		$\tau_{yz} = \frac{1}{2}\sqrt{2}\,\tau_r$ or $\sqrt{2}\,\tau_r$	$-\sqrt{2}\,C$	0	3	9	$-\frac{11\sqrt{2}C\tau_r}{24k\Theta}$

TABLE IX

					E[110]	E[1$\bar{1}$0]	E[001]	
	(01$\bar{1}$) [011]		$\sigma_x = 0$ or $2\tau_r$	$2A_1 - 2A_2 + 2B$	2	2	0	0[1$\bar{1}$0]:
	(011) [01$\bar{1}$]		$\sigma_y = 2\tau_r$ or 0	$2A_1 - 2A_2 - 2B$	0	0	4	$-\frac{3B\tau_r}{4k\Theta}$
[110]	or	$\frac{1}{4}\sigma$[110]	$\sigma_z = -2\tau_r$	$+ 4B$	1	1	2	
	(10$\bar{1}$) [101]		$\tau_{xy} = \tau_{xz} = \tau_{yz} = 0$	$- 4B$	1	1	2	
	(101) [10$\bar{1}$]			$-2A_1 + 2A_2 + 2B$	2	2	0	0[001]:
				$-2A_1 + 2A_2 - 2B$	2	2	0	0

TABLE X

axis of compression	slip system	shear stress τ	tensor elements σ_{ij}	energy shifts Δ	state of polarization E[110]	E[1$\bar{1}$0]	E[001]	zero-load polarization P_0
[110]	4 pairs of $\{1\bar{1}0\}\langle 110\rangle$	$\frac{1}{4}\sigma$[110]	$\sigma_x = \tau_r$ $\sigma_y = \tau_r$ $\sigma_z = -2\tau_r$ $\tau_{xy} = \tau_{xz} = \tau_{yz} = 0$	$-2A_1 + 2A_2$ $A_1 - A_2 + 3B$ $A_1 - A_2 - 3B$	1 1 0	1 1 0	0 0 2	0[1$\bar{1}$0]: $-\frac{9B\tau_r}{4k\Theta}$ 0[001]: 0

TABLE XI

axis of compression	slip system	shear stress τ	tensor elements σ_{ij}	energy shifts Δ	state of polarization E[110]	E[1$\bar{1}$0]	E[001]	zero-load polarization P_0
[110]	(101) [10$\bar{1}$] (10$\bar{1}$) [101] (011) [01$\bar{1}$] (01$\bar{1}$) [011]	$\frac{1}{4}\sigma$[110]	$\sigma_x = 2\tau_r$ $\sigma_y = 2\tau_r$ $\sigma_z = -4\tau_r$ $\tau_{xy} = \tau_{xz} = \tau_{yz} = 0$	$-4A_1 + 4A_2$ $2A_1 - 2A_2 - 6B$ $2A_1 - 2A_2 - 6B$	1 1 0	1 1 0	0 0 2	0[1$\bar{1}$0]: $-\frac{9B\tau_r}{2k\Theta}$ 0[001]: 0

TABLE XII

axis of compression	slip system	shear stress τ	tensor elements σ_{ij}	energy shifts Δ	state of polarization E[110]	E[1$\bar{1}$0]	E[001]	zero-load polarization P_0
[110]	one $\{001\}\langle 110\rangle$	$\frac{1}{4}\sqrt{2}\,\sigma$[110]	$\sigma_x = \sigma_y = \sigma_z = 0$ $\tau_{xy} = \frac{1}{2}\sqrt{2}\,\tau_r$ $\tau_{xz} = \tau_{yz} = 0$ or $\pm\frac{1}{2}\sqrt{2}\,\tau_r$	$-\frac{1}{2}\sqrt{2}\,C$ 0 $-\frac{1}{2}\sqrt{2}\,C$	5 2 1	1 2 5	2 4 2	0[001]: $-\frac{\sqrt{2}\,C\tau_r}{4k\Theta}$

TABLE XIII

axis of compression	slip system	shear stress τ	tensor elements σ_{ij}	energy shifts Δ	state of polarization E[110]	E[1$\bar{1}$0]	E[001]	zero-load polarization P_0
			$\sigma_x = \sigma_y = \sigma_z = 0$					
	two			$+\sqrt{2}\,C$	2	0	0	0[001]:
[110]	{001} ⟨110⟩	$\frac{1}{4}\sqrt{2}\,\sigma$[110]	$\tau_{xy} = \sqrt{2}\,\tau_r$	$+\frac{1}{2}\sqrt{2}\,C$	1	1	2	$-\dfrac{\sqrt{2}\,C\tau_r}{2k\Theta}$
			$\tau_{xz} = \pm\frac{1}{2}\sqrt{2}\,\tau_r$	$-\frac{1}{2}\sqrt{2}\,C$	1	1	2	
			$\tau_{yz} = \pm\frac{1}{2}\sqrt{2}\,\tau_r$	$-\sqrt{2}\,C$	0	2	0	

TABLE XIV

					E[110]	E[1$\bar{1}$0]	E[001]	
			$\sigma_x = \sigma_y = \sigma_z = 0$	$+\frac{3}{2}\sqrt{2}\,C$	4	0	0	
	three			$+\frac{1}{2}\sqrt{2}\,C$	1	1	2	0[001]:
[110]	{001} ⟨110⟩	$\frac{1}{4}\sqrt{2}\,\sigma$[110]	$\tau_{xy} = \frac{3}{2}\sqrt{2}\,\tau_r$	0	2	2	4	$-\dfrac{3\sqrt{2}\,C\tau_r}{4k\Theta}$
			$\tau_{xz} = 0$ or $\pm\frac{1}{2}\sqrt{2}\,\tau_r$	$-\frac{1}{2}\sqrt{2}\,C$	1	1	2	
			$\tau_{yz} = 0$ or $\pm\frac{1}{2}\sqrt{2}\,\tau_r$	$-\frac{3}{2}\sqrt{2}\,C$	0	4	0	

TABLE XV

					E[110]	E[1$\bar{1}$0]	E[00$\bar{1}$]	
			$\sigma_x = \sigma_y = \sigma_z = 0$					
	four			$+2\sqrt{2}\,C$	1	0	0	0[001]:
[110]	{001} ⟨110⟩	$\frac{1}{4}\sqrt{2}\,\sigma$[110]	$\tau_{xy} = 2\sqrt{2}\,\tau_r$	0	1	1	2	$-\dfrac{\sqrt{2}\,C\tau_r}{k\Theta}$
			$\tau_{xz} = 0$	$-2\sqrt{2}\,C$	0	1	0	
			$\tau_{yz} = 0$					

slip systems and column 3 the shear stress τ, with which these systems are stressed. τ is given by the well-known equation

$$\tau = \sigma \cos(\sigma, X') \cos(\sigma, Z'), \tag{15}$$

where (σ, X') is the angle between σ and the slip direction X' of a slip system, and (σ, Z') is the angle between σ and the slip plane normal Z'. Column 4 contains the tensor elements of the residual shear stress τ_r in the coordinate system of the cubic crystal axes. The residual shear stress τ_r of a slip system being directed along the Burgers vector, the tensor elements of the stress in the coordinate system of the cubic crystal axes can be easily found:

$$\sigma_{ij} = \{\cos(X', i) \cos(Z', j) + \cos(X', j) \cos(Z', i)\} \tau_r. \tag{16}$$

Substitution of the elements in eqs. 10 and 11 in the paper of Hughes and Runciman[3]) gives the energy shifts as given in column 5. With the same paper the state of polarization of the emitted radiation, column 6, may be derived. Finally, column 7 gives the polarization degree of the emitted radiation for an unloaded crystal. The magnitude of the residual stresses is unknown, the lowest and highest estimations diverge by two orders, depending on the measuring procedure[11,12]). We think a good choice will be to take the residual, internal stress equal to the difference between the resolved shear stress and the critically resolved shear stress:

$$\tau_r = (\sigma - \sigma_f) \cos(\sigma, X') \cos(\sigma, Z'). \tag{17}$$

This choice is supported by three considerations.

1. In the loaded crystal the stress is uniformly distributed over the crystal, as we observed with a polariscope. Thus all slip systems of the same kind are equally stressed.
2. The maximum value of the residual stress will be as high as the applied resolved shear stress, because KCl has a strong Bauschinger effect[8,11]) and on unloading and reloading no great difference in strength is observed[8]).
3. Below σ_f the residual stress is zero, from σ_f on it increases continuously. The residual shear stress is proportional to the total number of dislocations in the crystal, and the number of dislocations is dependent on the applied stress.

In the next paragraphs the calculations summarized in the tables are collated with the experimental results of figs. 3 and 4. The slip systems considered are $\{1\bar{1}0\}\langle 110\rangle$, generally accepted as primary system, and $\{1\bar{1}1\}\langle 110\rangle$ and $\{001\}\langle 110\rangle$ as secondary systems[11]). The active slip systems are mainly dependent on the stress direction but can also be influenced by the dimension of the sample: mostly slip is developed on the system having the shortest direction. This size effect is taken into account in the following.

σ[001]. The slip systems activated at low stress are, according to microscopic observations and because of the size effect, (101) [101] and (101) [$\bar{1}$01] (table I). If only one system is active, it follows that $\Delta P = P_\sigma - P_0 = P_\sigma$. If both systems are active simultaneously the energy shifts are twice as large, the polarization is the same. Thus, at the flow stress there will be no discontinuity, irrespective whether slip occurs on one or two systems.

At high stresses slip will occur on both oblique systems too (table II). The zero-load polarization is then $P_0 = 9B\tau_r/2k\Theta = 6\,a\tau_r$ and $\Delta P = P_\sigma - P_0 = a\sigma - 6a \times \frac{1}{2}(\sigma - \sigma_f) = -2a\sigma + 3a\sigma_f$.

This after oblique slip has set in ΔP will decrease, as has been found.

σ[111]. Experimentally, the results are the same whether the crystal is observed along [1$\bar{1}$0] or [11$\bar{2}$]. It seems reasonable to look for combinations of slip systems symmetrical with respect to [1$\bar{1}$0] and [11$\bar{2}$]. There are three combinations of three systems which possess this property:

(1$\bar{1}$1) [110]	($\bar{1}$11) [110]	(001) [110]
($\bar{1}$11) [101]	(11$\bar{1}$) [101]	(010) [101]
(11$\bar{1}$) [011]	(1$\bar{1}$1) [011]	(100) [011]

The first two combinations (table III) give a zero-load polarization

$$P_0 = -\frac{\sqrt{6}C\tau_r}{4k\Theta} = \sqrt{6}b\tau_r.$$

Then $\Delta P = P_\sigma - P_0 = b\sigma - \sqrt{6}b \times \frac{1}{9}\sqrt{6}(\sigma - \sigma_f) = \frac{1}{3}b\sigma + \frac{2}{3}b\sigma_f$.
Substitution of the experimentally found value of b (eq. 13) gives

$$\Delta P = -(3.2 \pm 0.5)\,\sigma \times 10^{-10} - (6.4 \pm 1.0)\,\sigma_f \times 10^{-10}.$$

The third combination (table IV) leads to

$$P_0 = -\frac{3\sqrt{2}C\tau_r}{4k\Theta} = 3\sqrt{2}b\tau_r$$

and

$$\Delta P = P_\sigma - P_0 = b\sigma - 3\sqrt{2}b + \tfrac{1}{3}\sqrt{2}(\sigma - \sigma_f) = -b\sigma + 2b\sigma_f.$$

The three combinations cannot account for the horizontal curves in fig. 3. So, apparently the assumption based upon the symmetry argument was not right. Combinations of more than three $\{\bar{1}11\}\langle 110\rangle$ systems which could provide a nearly horizontal curve are not likely, because of their complexity as is expressed by the complicated forms of the energy shifts and the zero-load polarization. In a third approach we calculated the effects of all possible combinations of $\{001\}\langle 110\rangle$ slip systems as given in tables V up to VIII. Although the results of the calculations (table XVI) do not predict

horizontal curves, the best explanation of the experiments is given by:

$0[1\bar{1}0]$:	(001) [110]	or	(100) [011]	and	(010) [101],	
$0[11\bar{2}]$:	(100) [011]	or	(010) [101]	or	(010 [101]	and
	(001) [110]	or	(100) [011]	and	(001) [110].	

For these slip systems ΔP *vs.* σ will show a small deviation from the horizontal lines drawn in fig. 3 which, however, remains within the uncertainty of the measurements. The data are insufficient to make a choice between the possibilities, but with the general rule that slip occurs on the system having the shortest slip distance, we may select the most probable systems. Being the longest dimension of the cross section of the samples always directed along the observation axis O, as drawn in fig. 2, the systems are:

$0[1\bar{1}0]$: (001) [110],
$0[11\bar{2}]$: (100) [011] or (010) [101].

$\sigma[110]$. As fig. 4 shows, the slip is very badly reproducible if the crystal is compressed along [110]. Let us first consider the case where the crystal was observed along $[1\bar{1}0]$. As we observed with the polariscope, slip occurs in this case on at least two primary slip systems. The two pairs (table IX)

$$\begin{matrix}(01\bar{1})\,[011] \\ (011)\,[01\bar{1}]\end{matrix} \quad \text{or} \quad \begin{matrix}(10\bar{1})\,[101] \\ (101)\,[10\bar{1}]\end{matrix}$$

cause a zero-load polarization $P_0 = -3B\tau_r/4k\Theta = -a\tau_r$ and

$$\Delta P = P_\sigma - P_0 = c\sigma + a \times \tfrac{1}{4}(\sigma - \sigma_f) = (c + \tfrac{1}{4}a)\,\sigma - \tfrac{1}{4}a\sigma_f.$$

As $(c + \frac{1}{4}a) < 0$ these two pairs of slip systems cannot explain the observed effects. The other four pairs (table X)

$$\begin{matrix}(101)\,[10\bar{1}] \\ (01\bar{1})\,[011]\end{matrix} \quad \begin{matrix}(10\bar{1})\,[101] \\ (011)\,[01\bar{1}]\end{matrix} \quad \begin{matrix}(10\bar{1})\,[101] \\ (01\bar{1})\,[011]\end{matrix} \quad \begin{matrix}(101)\,[10\bar{1}] \\ (011)\,[01\bar{1}]\end{matrix}$$

cause a zero-load polarization $P_0 = -9B\tau_r/4k\Theta = -3a\tau_r$ and

$$\Delta P = P_\sigma - P_0 = c\sigma + 3a \times \tfrac{1}{4}(\sigma - \sigma_f) = (c + \tfrac{3}{4}a)\,\sigma - \tfrac{3}{4}a\sigma_f.$$

We see that, as $(c + \frac{3}{4}a) = -(1 \pm 2) \times 10^{-10}\ \mathrm{m^2\ N^{-1}}$, these combinations can account for the nearly stress-independent measurements.

Finally, we have to consider the possibility that slip occurs on all four primary slip systems (table XI). The symmetry of the residual stress fields is the same above, and as the energy shifts are twice as great P_0 differs by a factor 2 from the last case. Thus $P_0 = -6a\tau_r$ and

$$\Delta P = P_\sigma - P_0 = c\sigma + 6a \times \tfrac{1}{4}(\sigma - \sigma_f) = (c + \tfrac{3}{2}a)\,\sigma - \tfrac{3}{2}a\sigma_f.$$

As $(c + \frac{3}{2}a) = (1.2 \pm 3) \times 10^{-10}\ \mathrm{m^2\ N^{-1}}$ all four primary slip systems together can explain the highest curves.

In all cases mentioned above P_0 is zero if the luminescence is observed along [001]. However, we observed a discontinuity at the flow stress, so other slip systems must be involved. As follows from the calculations along the same lines as have been followed for table IX up to XI, slip systems of the $\{\bar{1}11\}\langle 110\rangle$ type also lead to $P_0 = 0$ as the symmetry of the stress fields appears to be the same as that of the $\{1\bar{1}0\}\langle 110\rangle$ systems. Therefore, the only possibility is that $\{001\}\langle 110\rangle$ are active. If only one system (table XII) is active the zero-load polarization is $P_0 = -\sqrt{2}C\tau_r/4k\Theta = \sqrt{2}d\tau_r$ and

$$\Delta P = P_\sigma - P_0 = d\sigma - \sqrt{2}d \times \tfrac{1}{4}\sqrt{2}(\sigma - \sigma_f) = \tfrac{1}{2}d\sigma + \tfrac{1}{2}d\sigma_f.$$

As $\frac{1}{2}d = -(4.8 \pm 0.8) \times 10^{-10}\ \mathrm{m^2N^{-1}}$ the two lowest lying curves may be caused by one slip system. Two slip systems of the type $\{001\}\langle 110\rangle$ (table XIII) cause a zero-load polarization $P_0 = -\sqrt{2}C\tau_r/2k\Theta = 2\sqrt{2}d\tau_r$ and

$$\Delta P = P_\sigma - P_0 = d\sigma - 2\sqrt{2}d \times \tfrac{1}{4}\sqrt{2}(\sigma - \sigma_f) = d\sigma_f.$$

So, both horizontal curves can be explained by the occurrence of two such slip systems. Three slip systems (table XIV) lead to

$$P_0 = -3\sqrt{2}C\tau_r/k\Theta = 3\sqrt{2}d\tau_r$$

and

$$\Delta P = P_\sigma - P_0 = d\sigma - 3\sqrt{2}d \times \tfrac{1}{4}\sqrt{2}(\sigma - \sigma_f) = -\tfrac{1}{2}d\sigma + \tfrac{3}{2}d\sigma_f.$$

So, the rising curves can be explained with three slip systems. A curve to be explained by four slip systems (table XV) we observed once, as will be mentioned in the discusssion.

TABLE XVI

slip systems			zero-load polarization P_0	
			$0[1\bar{1}0]$	$0[11\bar{2}]$
(100) [011],	(010) [101],	(001) [110]	$2b(\sigma - \sigma_f)$	$2b(\sigma - \sigma_f)$
(010) [101],	(001) [110]		$\frac{13}{9}b(\sigma - \sigma_f)$	$\frac{11}{9}b(\sigma - \sigma_f)$
(100) [011],	(001) [110]		$\frac{13}{9}b(\sigma - \sigma_f)$	$\frac{11}{9}b(\sigma - \sigma_f)$
(100) [011],	(010) [101]		$\frac{10}{9}b(\sigma - \sigma_f)$	$\frac{14}{9}b(\sigma - \sigma_f)$
(001) [110]			$\frac{8}{9}b(\sigma - \sigma_f)$	$\frac{4}{9}b(\sigma - \sigma_f)$
(100) [011]			$\frac{5}{9}b(\sigma - \sigma_f)$	$\frac{7}{9}b(\sigma - \sigma_f)$
(010) [101]			$\frac{5}{9}b(\sigma - \sigma_f)$	$\frac{7}{9}b(\sigma - \sigma_f)$

4. *Discussion.* In the preceding section more or less reproducible curves are given. We measured other curves too, appearing only once in our observations. Apparently, they are of a more complicated character. In fig. 6 two such curves are shown. The $\sigma[111]$, $0[1\bar{1}0]$ curve is easy to explain.

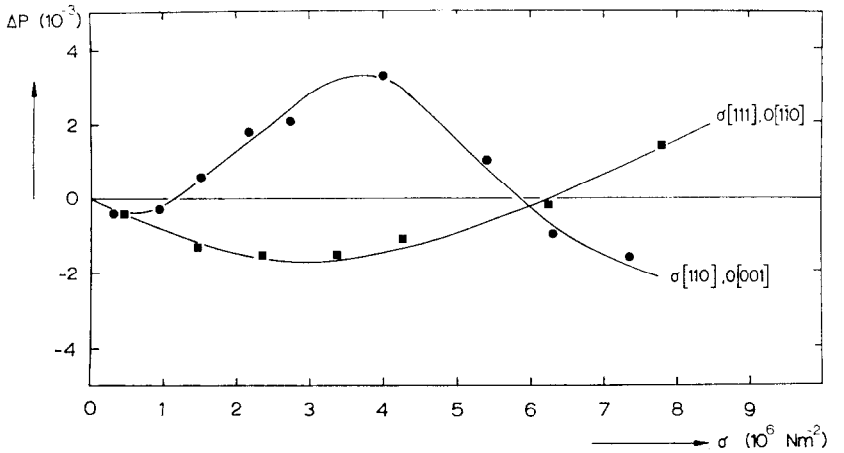

Fig. 6. Two peculiar piezospectroscopic curves with a more complicated character than the curves in figs. 3 and 4.

After the usual decrease in the elastic region the curve rises again with the same slope. ΔP calculations based upon tables V up to VIII and XVI prove that all three $\{001\}\langle 110\rangle$ systems are active simultaneously. The second curve, *i.e.* $\sigma[110]$, $0[001]$, shows a hump. After the elastic region the curves rise, this can be calculated from slip on all four $\{001\}\langle 110\rangle$ systems (table XV). At about 4×10^6 N m^{-2} the polarization decreases again just as in the elastic region. As is shown slip on $\{1\bar{1}0\}\langle 110\rangle$ does not lead to a zero-load polarization for $0[001]$. Apparently, slip is started on $\{001\}\langle 110\rangle$, later on these systems became inactive, and for some unknown reason slip is continued on $\{1\bar{1}0\}\langle 110\rangle$.

The elastic region of the second curve is very small. We frequently observed that the elastic region was absent completely. This must be due to stresses already present in the crystal before the experiment has started. The polarization effect turned out to be very sensitive to the initial state of stress.

The poor reproducibility of the curves as a whole is mainly due to varying factors inducing irreversible slip in the various slip systems of the crystals. The deviation of each measuring point from the drawn, mediate curve may be caused by the discontinuous flow of the crystal, resulting in a stress-strain curve of the stair-step type[16]).

Let us compare the slip systems found by us with the slip systems mentioned in the literature.

$\sigma[001]$. This is the only stress direction for which the slip systems are well known[13]). The systems are of the type $\{1\bar{1}0\}\langle 110\rangle$, four of the six systems are stressed. In the easy glide region slip occurs preferentially on two orthogonal slip systems, both systems may be active simultaneously but frequently one of them becomes inactive after the samples

slipped to a certain amount. In stage II the crystal also slips on the oblique third and fourth systems. Our observations are in accordance with these inferences completely.

$\sigma[111]$. The observations mentioned in the literature about the slip systems activated by this stress direction are rather poor. Schmid and Boas[11]) cite some older authors from before the second World War. More recently Matucha[14]) published some observations: The primary $\{1\bar{1}0\}\langle 110\rangle$ systems are unstressed, mainly $\{001\}\langle 110\rangle$ the systems are activated, $\{1\bar{1}1\}\langle 110\rangle$ are also found but in very localized regions. We observed the main $\{001\}\langle 110\rangle$ systems.

$\sigma[110]$. A [110] stress is reported to activate primary $\{1\bar{1}0\}\langle 110\rangle$ and secondary $\{1\bar{1}1\}\langle 110\rangle$ or $\{001\}\langle 110\rangle$ slip systems[14,15]). We found primary $\{1\bar{1}0\}\langle 110\rangle$ and secondary $\{001\}\langle 110\rangle$ systems. This in accordance with the observations of Matucha[14]), that $\{1\bar{1}1\}\langle 110\rangle$ is found only in very restricted regions of the samples.

Generally, we may put that our observations are in agreement with the outlines of the newer litterature. The experimental method used here has the additional advantage to yield the particular slip systems involved.

Many piezospectroscopic investigations are made with such high stresses that plastic deformation must have taken place. Nevertheless, in every case, as far as we know, the impression is given and the measurements are explained as if the deformation is elastic only. The very reason is that no difference can be seen in the stress distribution in a loaded crystal before and after plastic deformation. However, in the present investigation there is a marked difference between the effects in the elastic and the plastic region due to the experimental implementation used.

Recapitulation. On the basis of the analysis of the piezospectroscopic measurements the mechanical behaviour of KCl is as follows.

1. If the uniaxial stress is applied along [100] the frequently observed $\{1\bar{1}0\}\langle 110\rangle$ systems are stressed. In general, at low stresses one or two of the four stressed systems are active (orthogonal slip), at high stresses all four systems are active (oblique slip).
2. If the uniaxial stress is applied along [111] it is highly probable that one of the three stressed $\{001\}\langle 110\rangle$ systems is active.
3. A uniaxial stress along [110] can produce slip in many different ways. If the sample has a nearly quadratic cross section two or four $\{1\bar{1}0\}\langle 110\rangle$ systems are active, if the sample is of uncommon shape it is possible to force slip on one, two, three, or even four $\{001\}\langle 110\rangle$ systems.
4. Finally, we may conclude that the piezospectroscopic investigation of impurity centres is a useful tool not only in determining the symmetry of the centres itselves, but also in revelation of the slip systems activated by the stress.

Acknowledgement. This investigation was part of the research programme of the "Stichting voor Fundamenteel Onderzoek der Materie", and was made possible by financial support from the "Nederlandse Organisatie voor Zuiver-Wetenschappelijk Onderzoek".

REFERENCES

1) Koeze, P. and Volger, J., Physica **37** (1967) 467.
2) Kaplyanskii, A. A., Optics and Spectrosc. **16** (1964) 329, 557.
3) Hughes, A. E. and Runciman, W. A., Proc. phys. Soc. **90** (1967) 827.
4) Sibley, W. A., Sonder, E. and Butler, C. T., Phys. Rev. **136** (1964) A537.
5) Grailich, J., Krystallographisch-optische Untersuchungen, Thesis, Wien (1858).
6) Koeze, P., Thesis, Utrecht (1968).
7) Föppl, L. and Mönch, E., Praktische Spannungsoptik (Berlin, 1959).
8) Van Bueren, H. G., Imperfections in crystals (Amsterdam, 1960).
9) Haven, Y. and Van Santen, J. H., Nuovo Cimento Suppl. **7** (1958) 605.
10) Burnstein. E., Davisson, J. W. and Sclar, N., Phys. Rev. **96** (1954) 819.
11) Schmid, E. and Boas, W., Plasticity of crystals (London, 1950).
12) Mendelson, S., J. appl. Phys. **32** (1961) 1999.
13) Davidge, R. W. and Pratt, P. L., Phys. Status solidi **6** (1964) 759.
14) Matucha, K. H., Phys. Status solidi **26** (1968) 291.
15) Hosford, W. F., Chao, H. C. and Van Vlack, L. H., Trans. Metall Soc. AIME **236** (1966) 1574.
16) Okada, T. and Suita, T., Tech. Rep. Faculty Engng. Osaka Univ. **16** (1965) 265.